A Leukocyte Detection Technique in Blood Smear Images Using Plant Growth Simulation Algorithm

Deblina Bhattacharjee, Anand Paul*

The Graduate School of Computer Science and Engineering,
Kyungpook National University, Daegu, South Korea
deblina0210@knu.ac.kr, anand@knu.ac.kr*

Abstract

For quite some time, the analysis of leukocyte images has drawn significant attention from the fields of medicine and computer vision alike where various techniques have been used to automate the manual analysis and classification of such images. Analysing such samples manually for detecting leukocytes is time-consuming and prone to error as the cells have different morphological features. Therefore, in order to automate and optimize the process, the nature-inspired Plant Growth Simulation Algorithm (PGSA) has been applied in this paper. An automated detection technique of white blood cells embedded in obscured, stained and smeared images of blood samples has been presented in this paper which is based on a random bionic algorithm and makes use of a fitness function that measures the similarity of the generated candidate solution to an actual leukocyte. As the proposed algorithm proceeds the set of candidate solutions evolves, guaranteeing their fit with the actual leukocytes outlined in the edge map of the image. The experimental results of the stained images and the empirical results reported validate the higher precision and sensitivity of the proposed method than the existing methods. Further, the proposed method reduces the feasible sets of candidate points in each iteration, thereby decreasing the required run time of load flow, objective function evaluation, thus reaching the goal state in minimum time and within the desired constraints.

Introduction

Out of the numerous fields where nature-inspired methods have been applied to solve pressing problems, medical image processing is one such field where bionic methods have been used invariably, especially focused on object detection. In this paper, the problem of leukocyte detection in blood smear images has been solved where the highly efficient PGSA (Tong et al. 2005) has been applied for the automated analysis and classification of white blood cell (WBC) from such images. WBCs or leukocytes, hold paramount significance in the diagnosis of a number of diseases. However, performing the WBC tests and analysing them manually is tough and requires highly skilled and experienced haematologists. As such highly labour intensive routine procedures have an increased possibility of an intra and inter-observer variability, new ways for cell analysis are being formed using digital image processing techniques to develop more reliable systems for disease diagnosis. In addition to it, the cell differentials vary with respect to their shape, features, contrast between cell boundaries and background, positions and size which pose as further challenges for leukocyte detection. As WBCs are quasi-circular in shape, the problem of their detection in smear images has been solved in context of a circle detection task in this paper. Interestingly, detecting circular features in medical images are extremely important with a broad scope extending from blood cells to ovarian cells and liver cells (Karkavitsas and Rangoussi 2007) and this problem has been solved using PGSA in this article. PGSA having been introduced in the year 2005 (Tong et al. 2005) has never been applied to image processing techniques before. The PGSA based circle detector randomly selects three points representing the candidate circles on the edge pixel map of the smear image. Upon validation of the existence of the candidate solution on the edge map, a fitness function is used to measure the resemblance between the candidates with the actual WBCs. The set of candidate solutions evolve via successive iteration of PGSA based on the values of the fitness function such that they can fit into the actual WBC on the image. The approach forms a subpixel detector that can effectively identify leukocytes in real images. Thus, this paper uses the highly efficient PGSA by proposing a new leukocyte detector algorithm that optimally recognizes leukocytes under varied complex conditions solved as a circle detection problem.

Background

As per the existing conventional method of Hough Transform for circle detection in digital images (Muammar

and Nixon 1989), to cover the parameters of the origin coordinates and the radius of the circle (x, y, r), a lot of memory is required. It also implies a high computational time complexity decreasing its processing speed. Also, the method is not resistant to noise thereby resulting in even lower accuracy (Atherton and Kerbyson 1993). To overcome such a problem, some other approaches based on the Hough transform, for instance the probabilistic Hough transform (Shaked et al. 1996), Circular Hough transform with local maximization (Yadav et al. 2014), one-dimensional Hough Transform (Zhou et al. 2014), Hough Transform of curves (Campi et al. 2013) and recently scanline-based hybrid Hough Transform (Seo and Kim 2015) have been proposed with better time complexities but having average memory usage and no noise resistance. In order to overcome the drawbacks of the Hough Transforms, many optimization techniques have been applied to the circle detection problem. These methods have produced much higher accuracy, stability, computational speed and robustness as compared to the discussed Hough Transform as well as other methods like Otsu method based on circular histogram (Wu et al. 2006), support vector machines (Wang and Chu 2009), and modified transformation method (George et al. 2014). These optimization techniques are nature-inspired methods all of which has been discussed in context of solving the circle detection problem hereunder.

In summary, the genetic algorithm (GA) is the most favoured computational intelligence model for multi-circle detection (Ayala-Ramirez et al. 2006). However, due to the nature of global optimization of genetic algorithm, multi-circle detection requires additional processing. In (Das et al. 2008), simulated annealing and differential evolution has been combined to perform circle detection. Although the method here is robust to noise, it fails to detect circle locations with considerable precision, under both clear and noisy conditions seen from their result samples. In ant colony algorithm (Chattopadhyay et al. 2008), the final circle detection criterion is to threshold the deviation error derived from the detected radius which is the distance between corresponding edge pixels and circle centre. This method is essentially a closed loop tracking method, and its performance is questionable when circular shape edges are not enclosed. In (Cuevas et al. 2012), where the artificial bee colony algorithm has been used, the potential problem is that a lot of memory space would be used if the iteration is set to a large number, but it saves rerun computations. For the fuzzy cellular neural network (Wang et al. 2007), the basic limitation is that it takes single inputs where only one WBC is analysed. Moreover, with an exponential increase in the number of iterations the detected circle gets distorted covering the surrounding area, thereby giving more false positives and losing out on the true positives. In the clonal selection algorithm for circle detection (Isa et al. 2010), both the antigens and antibodies are designed as 10-by-10 images and representations are a binary string which makes it not very practical to process normal resolution images. In this paper, the detection of WBC has been done by the PGSA. In the literature (Wang and Cheng 2007), PGSA is compared with other optimization algorithms where the results have shown that the optimal network given by PGSA is the best option as compared to the existing optimization techniques namely GA, particle swarm optimization, gradient descent and Tabu search, with a higher rate of accuracy and faster global optimization. As per the analyses, PGSA has the following advantages: 1. the objective function and constraint satisfaction are dealt separately 2. it does not require any predefined error coefficient, rates of cross-over and mutation therefore resulting in stable solutions 3. it has a search mechanism with ideal direction and randomness balancing property which finds the global optimal solution quickly. Thus, PGSA gives minimum loss while showing greater convergence stability.

Proposed Scheme: Circle Detection using PGSA

Plant Growth Simulation Algorithm (PGSA)

The PGSA is a bionic random algorithm guided by plant phototropism (the ability of a plant to bend towards the light source). The light source is the global optimal solution and the PGSA simulates the mechanism of plant phototropism by assessing the morphactin concentration on the growth points of the plant. This morphactin concentration decides the growth and is dependent on the intensity of light. The algorithm emphasises on a plant system's method of making decisions which are based on plant's growth rules and probability models (Bhattacharjee and Paul 2016).

Mathematical Model for Plant Growth

According to the probability model of PGSA, *f(i)* is the fitness function for the node *i* on the plant to grow in the given environment. The biological laws of plant growth specifies that if the value of *f(i)* is smaller, then node *i* has a better environment for growing into a new branch. The mathematical model of PGSA is as follows. Given a root R_0, a trunk T grows from the root. Assuming that there are n nodes on the trunk T that might provide a more thriving growth environment than the root, i.e. the fitness function $f(R_{Ti}) < f(R_0)\ (i = 1,2,\dots,n)$, the morphactin concentrations C_{Ti} of these nodes are shown in equation (1).

$$\boldsymbol{C_{Ti} = \frac{f(R_0)-f(R_{Ti})}{\sum_{i=1}^{n}(f(R_0)-f(R_{Ti}))}} \quad \textbf{(i=1,2,…,n)} \qquad \textbf{(1)}$$

The above equation shows that the morphactin concentration of a node in a plant is dependent on the growth environment of all the nodes on the plant. A change in the concentration of one node, therefore effects the rest. These concentrations can be imagined as a state space of the interval [0, 1] because the $\sum C_{Ti}$=1. The state space can be shown as in Figure 1.

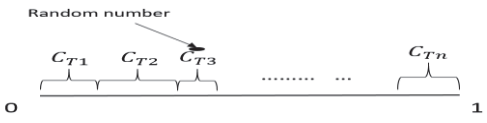

Figure 1: Morphactin concentration space

Now, from the state space of concentrations a random number is obtained which returns a random concentration C_{TM}. The corresponding preferential node R_{TM} takes the priority in the next iteration to branch out. However, the node R_{TM} will grow into a branch only if the random number β satisfies the following two conditions in equations (2) and (3).

$$\mathbf{0} \leq \boldsymbol{\beta} \leq \sum_{i=1}^{M} \boldsymbol{C_{Ti}} (\boldsymbol{M = 1}) \quad \textbf{(2)}$$

$$\sum_{i=1}^{M-1} \boldsymbol{C_{Ti}} < \boldsymbol{\beta} \leq \sum_{i=1}^{M} \boldsymbol{C_{Ti}} (\boldsymbol{M = 2, 3, \ldots, n}) \quad \textbf{(3)}$$

After the branch sprouts out, the morphactin concentration of the current node, R_{TM}, is set to zero and the morphactin concentration of the remaining nodes is reallocated as follows:

$$\boldsymbol{C_{Ti}} = \frac{f(\boldsymbol{R_0}) - f(\boldsymbol{R_{Ti}})}{\sum_{i=1, i \neq M}^{n} \left(f(\boldsymbol{R_0}) - f(\boldsymbol{R_{Ti}})\right) + \sum_{j=1}^{p} \left(f(\boldsymbol{R_0}) - f(\boldsymbol{R_{bj}})\right)} \quad \textbf{(4)}$$

$$\boldsymbol{C_{bj}} = \frac{f(\boldsymbol{R_0}) - f(\boldsymbol{R_{bj}})}{\sum_{i=1, i \neq M}^{n} \left(f(\boldsymbol{R_0}) - f(\boldsymbol{R_{Ti}})\right) + \sum_{j=1}^{p} \left(f(\boldsymbol{R_0}) - f(\boldsymbol{R_{bj}})\right)} \quad \textbf{(5)}$$

After the reallocation of the concentrations to all the nodes on the plant except R_{TM}, the state space of concentrations is again formed with the same interval [0, 1]. Assuming, the newly grown branch b has p nodes, such that $f(R_{bi}) < f(R_0)$ $(i = 1,2, \ldots, p)$, again a random number β is thrown in the state space and a new node branches out in the next iteration. The new state space has greater number of nodes now, i.e. the nodes previously present (n nodes) and the nodes on the new branch b (p nodes). This growth process stops in the bionic world when the plant has reached its maturity and cannot further branch out.

The PGSA has huge potential to be used in optimization problems. Here, the parameters are the fitness function (*f(i)*), the initial solution (root), search domain of candidate solutions (length of the trunk and branches) and candidate solutions (plant nodes). Further, it has a well-balanced exploration to exploitation ratio (Crepinsek et al. 2013). This method keeps exploring the entire search space with random node selection in the search interval [0, 1]. Although, candidate solutions (nodes) grow in each iteration the search space still remains in the interval [0, 1]. After the exploration, upon the selection of the best candidate solution (preferential node), the morphactin concentrations are reassigned by a neighbourhood like search that assesses the nodes in the vicinity of the just grown branch. The morphactin is not only assigned to the nodes on the new branch by exploitation but also to the previous nodes on the trunk by exploration in a given iteration. This is mainly because the objective function (growth environment) is dependent on the concentration of all the nodes on the plant. Thus PGSA has a well-balanced exploration to exploitation ratio which is necessary for any search optimization algorithm. Our approach is to use the above efficient naturally occurring technique to solve the leukocyte detection problem the overview of which is presented in Figure 2.

Data Preprocessing

To employ the proposed scheme with respect to leukocyte detection, the smear images are pre-processed to obtain two new images 1) The segmented image and 2) The edge pixel map of the segmented image. For the segmentation pre-processing part, the WBCs are isolated from other structures including red blood cells and the background pixels. Information of colour, brightness, and gradients are used with a corresponding threshold to generate classes to classify each pixel. A histogram thresholding method has been incorporated to segment the WBCs.

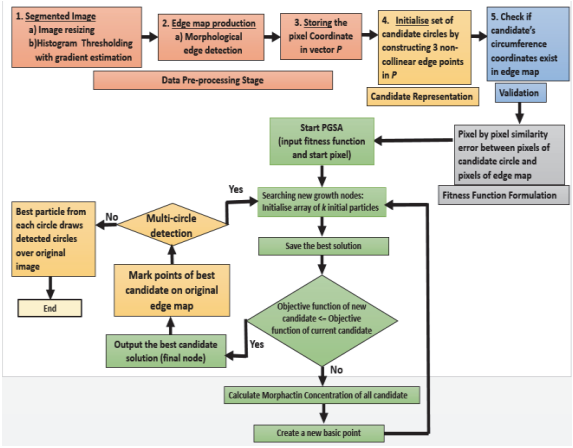

Figure 2. Detailed Process of WBC Detection from Smear Images

Now that the segmentation is done, the corresponding edge map is produced. The edge map maintains the total object structure while being just a simple representation of the original image. There are many different methods to detect the edges, but for our work the morphological edge detection procedure has been used (Zhaoxia and Han 2012) where erosion followed by inversion of the original image is carried out to ultimately compare it pixel-by-pixel with the original image. This results in the detection of pixels which are present in both the images. Thereafter, the (x_i, y_i) coordinates for every pixel p_i defining the image edge is stored in the image edge pixel vector P = $\{p_1, p_2, \ldots, p_{Np}\}$ with N_p being the total number of pixels defining the edge of the analysed image.

Particle Representation for Candidate Solutions

For the implementation of the algorithm the set of candidate solutions needs to be initialized. For this purpose, the circle candidates need to be constructed using the three non-collinear points on the edge of the circle, previously stored in the vector P. The indices which represent three edge pixel points are grouped assuming that the circle's contour map connects them together. Let the indices be $e_i, i = \{1,2,3\}$, then the circle $\boldsymbol{C}$ passing through these points can be the potential candidate solution for the circle detection problem. $\boldsymbol{C}= \{p_{e_1}, p_{e_2}, p_{e_3}\}$. The centre and radius of the circle $\boldsymbol{C}$ are given by the well-known second degree equation as seen in Equation (6).

$$(\boldsymbol{x} - \boldsymbol{x_0})^2 + (\boldsymbol{y} - \boldsymbol{y_0})^2 = \boldsymbol{r^2} \quad \textbf{(6)}$$

Therefore, a set of parameters is represented for each circle $[x_0, y_0, r]$ as a transformation T for all edge vector indices e_1, e_2, e_3 which yields:

$$[\boldsymbol{x_0}, \boldsymbol{y_0}, \boldsymbol{r}] = \boldsymbol{T}(\boldsymbol{e_1}, \boldsymbol{e_2}, \boldsymbol{e_3}) \quad \textbf{(7)}$$

By considering each index as a particle in the search space, the continuous search space is explored by using PGSA for a lookup of circle parameters $[x_0, y_0, r]$.

Fitness Function for the circle detection problem

Firstly, it is necessary to validate whether the circumference coordinates of the candidate circle $\boldsymbol{C}$ exists in the edge image. Upon this validation, the fitness function can be calculated. The coordinates spanning the circle circumference are $J = \{j_1, j_2, \dots, j_N\}$, where N is the total number of pixel points used for validating the circle coordinates. Thereafter, the fitness function $f(\boldsymbol{C})$ is defined as the pixel by pixel similarity error between the above set of pixels J of the circle candidate $\boldsymbol{C}$ (particle) and the pixels of the edge map, giving a greater fitness value for a higher resemblance. This function is given as follows,

$$\boldsymbol{f(C)} = \boldsymbol{1} - \frac{\sum_{i=1}^{N} \boldsymbol{E(j_i)}}{\boldsymbol{N}} - \frac{\boldsymbol{W_p}}{\boldsymbol{B_p}} \quad \textbf{(8)}$$

Where, $E(j_i)$ is the expectation function of the presence of the candidate circle pixel at j_i. Thus, $E(j_i)$ has maximum value of 1 if the pixel j_i is an edge pixel point. For all other pixel points, the expectation function has a zero value. Also, W_p is the amount of white pixel falling inside the candidate circle represented by $\boldsymbol{C}$ and B_p is the amount of black pixels falling inside $\boldsymbol{C}$ (Cuevas et.al. 2012). These two parameters have been taken into the calculation of the objective function as analysis of smear images cannot be done by directly applying the PGSA to such images. Smear images present different imaging conditions and staining intensities, which result in noisy edge maps. Thus, in order to use PGSA based circle detector within the context of WBC detection, the fitness function requires these parameters.

PGSA Implementation

The PGSA has the following steps.

Step 1. The edges are found and stored in the vector P as discussed in the pre-processing step. The iteration index is set to 1.

Step2. k initial particles are generated $(\boldsymbol{C}_{a,iteration=1}, a \in [1.\mathrm{k}])$ in the plant growth environment state space.

Step 3. The fitness function $f\left(\boldsymbol{C}_{a,iteration=i}\right)$ is evaluated to find the best candidate solution like R_{TM} as mentioned in the PGSA discussion in the previous section. This best candidate solution is named as $\boldsymbol{C}^{best} \leftarrow \arg\min\{f\left(\boldsymbol{C}_{a,iteration=i}\right)\}$.

Step 4. As per the PGSA discussed, the morphactin concentration at each of these particles (nodes) is checked as per equation (1). The particle with the higher morphactin concentration has a higher probability to move to the next iteration as an evolved candidate solution.

Step 5. The new branch position, which is the new particle's position is stored and the morphactin concentrations of all the particles are calculated again according to equation (4) and equation (5) except for $\boldsymbol{C}^{best}$ as it is the current local optimum solution.

Step 6. For every new particle, a maximum number of q particles are generated as per $j= 1, 2,\dots,q$ and based on the newly calculated morphactin concentration in *Step 5*, the new best candidate is found on the current generated branch in the previous step. This accounts for a neighbourhood like search for optimal candidate solutions. This process of generating new candidate solutions continues till a better minimized objective function is achieved and stops till there is no improvement in the fitness value of the generated candidate solutions.

Step 7. The set of all nodes that have branched out are the possible candidate solution with the final node $\boldsymbol{C}^{best}$ being the global best solution and others the local optimal solutions.

Step 8. From the original edge map, the algorithm marks the points corresponding to $\boldsymbol{C}^{best}$. In case of multi-circle detection it jumps to *Step 2*.

Step 9. Finally, the best particle $\boldsymbol{C}_{N_c}^{best}$ from each circle is used to draw (over the original image) the detected circles, where N_c is the number of circles detected.

Experimental Results

The proposed method for the detection of WBC was tested over 80 microscopic images of blood smear with a resolution of 360 x 363 pixels. The images that were used for the experiments had several deformities, occlusions and overlaps with other images that pose a significant challenge for the circle detection. Figure 3(a) shows an input blood smear image sample tested with the proposed method. Figure 3(b) shows the segmented WBCs obtained by histogram transforming. Figure 3(c) is the edge map of the segmented image and Figure 3(d) gives the detected WBCs.

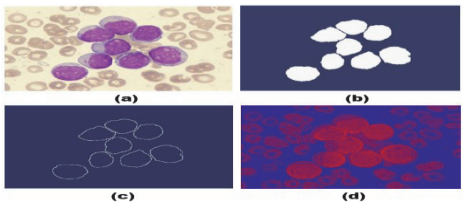

Figure 3. Resultant images of the first test on the application of the WBC detector (a) original image, (b) segmented image, (c) image edge map, and (d) the final result.

The proposed algorithm is tested on further complicated smear images. It represents an example with an image of deformed cells where detecting true circles becomes tougher. Despite such imperfections, the proposed approach can effectively detect the cells as it is shown in Figure 4(d).

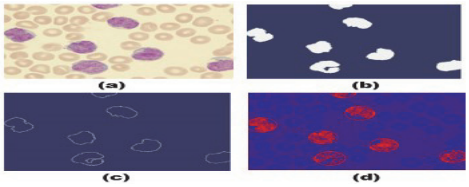

Figure 4. Resultant images of the second test on the application of the WBC detector for a complex and deformed image (a) original image, (b) segmented image, (c) edge map, and (d) the final result.

Further, the proposed scheme was tested for detecting partial or hidden leukocytes in blood smear images which are utmost challenging for any detection method. Although, the problem is complex in nature, PGSA is seen to be quite successful in detecting such leukocytes. The result is shown in Figure 5. However, the leukocytes that were detected were partially visible with 68% hidden surface. Such detections of completely hidden leukocytes will be part of the future scope of this paper.

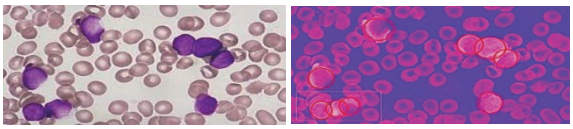

Figure 5: Resultant images of the third test on the application of the WBC detector for a complex image with partially hidden and deformed cells a) Original Image b) Result Image

Thus, the proposed method can successfully detect damaged, complex and partially hidden leukocytes correctly.

The dataset of smear-blood test images for evaluating the proposed scheme is downloaded from the website Cellavision.com which includes 80 images in JPG format of size 360 x 363 pixels, with a resolution of 10 pixels per 1µm. These images were medically graded and had 463 white blood cells (256 bright leukocytes and 207 dark leukocytes as per the blood smear conditions), all detected by a haematologist- a human medical expert. These numbers were taken as graded standards for all experimentations. For testing the proposed scheme over these images, the true positive rate (known as the number of correctly detected leukocytes over the number of leukocytes detected by the expert) and the false positive rate (known as the number of non-leukocytes that have been wrongly identified as leukocytes over the number of leukocytes which have been actually detected by the medical expert) have been evaluated. The results of the experiments show that the proposed method, achieves 98.28% leukocyte true positive rate with 1.72% false positive rate, and is therefore, arguably better than the other existing methods. To establish this statement, the proposed scheme has been further discussed and compared with other existing methods in context of the leukocyte detection problem.

Discussion

The circle detection problem can be considered as a binary classification task and hence, can be represented as a confusion matrix having the classes as 1) True Positives for correctly detected circles; 2) False Positives or wrongly detected circles; 3) True Negatives or non-circles correctly detected as such and 4) False Negatives or true circles wrongly labelled as non-circles. According to the circle detection task, the circle can be either a true positive, a false positive or a false negative, i.e. it can be correctly detected, incorrectly detected or undetected. Thus there is no true negative in a circle detection task as true negatives would have given non-detections of non-circles which is not of interest as it is a detection problem to begin with. Based on the confusion matrix, performance indices like true positive rate, false positive rate, false discovery rate and positive predictive value of the proposed algorithm are analysed. For this the dataset of 80 images from Cellavision was used to identify both bright and dark leukocytes using our proposed scheme. The results of such detections are shown in Table 1. All the analysed performance indices have been compared among four algorithms like Hough transform- HT (representing the traditional method), modified genetic algorithm with ant colony optimization- GA+ACO (both GA and swarm intelligence method are analysed here), fuzzy cellular neural network-FCCN (which is a member of neural networks) and the proposed method of PGSA. All the four algorithms perform the same data pre-processing and are applied by maintaining their original parameters. Thus, the performance comparison of all the methods are done based only on different blood smear images with varying background and target object conditions. These resultant images are then checked for established gold standards or medically graded standards by medical experts.

Table 1: Comparative performance of HT, FCCN, GA+ACO and PGSA for leukocyte detection

LEUKOCYTE TYPE	METHOD	LEUKOCYTES DETECTED(TRUE POSITIVES)	MISSING LEUKOCYTES (FALSE NEGATIVES)	WRONGLY DETECTED LEUKOCYTES (FALSE POSITIVES)	TRUE POSITIVE RATE	FALSE POSITIVE RATE	FALSE DISCOVERY RATE	POSITIVE PREDICTIVE VALUE
BRIGHT LEUKOCYTE (256)	HT	135	121	67	46.85%	30.18%	59.90%	66.83%
	FCCN	206	50	55	78.83%	24.77%	19.16%	78.93%
	GA+ACO	217	39	42	83.78%	18.92%	15.06%	83.78%
	PGSA	242	14	10	98.01%	1.99%	5.56%	96.03%
DARK LEUKOCYTE (207)	HT	100	107	54	48.04%	26.47%	69.48%	64.94%
	FCCN	168	39	49	81.37%	24.02%	17.97%	77.42%
	GA+ACO	183	24	38	88.72%	18.63%	10.86%	82.81%
	PGSA	202	5	6	98.55%	1.45%	2.40%	97.12%
OVERALL (463)	HT	235	228	121	47.42%	28.40%	64.04%	66.01%
	FCCN	374	89	104	80.05%	24.41%	18.62%	78.24%
	GA+ACO	400	63	80	86.15%	18.78%	13.13%	83.33%
	PGSA	444	19	16	98.28%	1.72%	4.13%	96.52%

From Table 1, we see that the PGSA has a detection rate of 98.28 % and is highly efficient when compared to other circle detection algorithms. The ROC curve of the True Positive Rate vs the False Positive Rate in Figure 6 below shows the detection rate of the proposed algorithm as reported in Table 1.

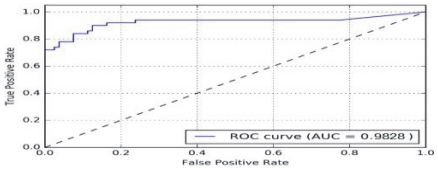

Figure 6. ROC Curve of the True Positive Rate vs the False Positive Rate in the proposed method

The results are further analysed with the help of other statistical performance metrics like precision and sensitivity as shown in Figure 7.

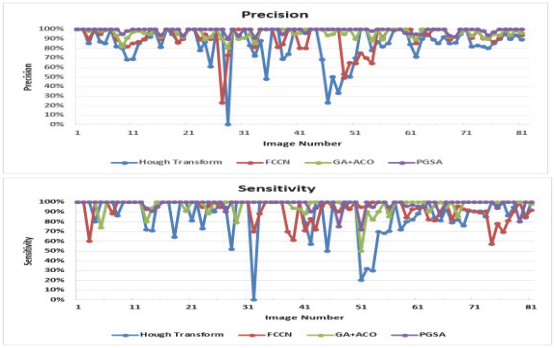

Figure 7. The (a) Precision and (b) Sensitivity graphs for the detection of true positives by all the four algorithms.

From figure 7, it is clear that HT has the least precision due to increased false detections with many images. The GA+ACO and PGSA are seen to achieve correct detection above 90% with small standard deviation, which are superior to the FCCN. The possible problem with the FCCN is that it requires a lot of computational time and memory to train its network and the detection is achieved over a large number of generations. Also, when the number of iterations increases, the possibility to cover other structures increases.

Sensitivity evaluates the detection rate over all existing circular shapes. On one hand, a low sensitive setting would result in good precision because detected circles must be true and distinctive, while sensitivity rate would be low because non-perfect shapes are missing. On the other hand, high sensitivity means reducing missing incidence but increasing the false detection rate at the same time. The PGSA model initializes nodes on all edge segments, which gives an almost perfect 100% overall sensitivity, due to every edge segment being checked for constraint satisfaction during each iteration as seen in Figure 7(b).

The proposed algorithm was also tested for its resistance towards noise. For this, the images from the used dataset were corrupted using the 1) Gaussian noise 2) Salt and pepper noise, which are the most pedestrian noise found in smear images of blood samples. All the 80 images were corrupted with these two noise types and were analysed by applying the four algorithms. The Gaussian noise level was used at $\sigma = 10$ and the salt and pepper noise level was used at 10%. The performance of these algorithms are shown in Table 2 and Table 3 respectively.

Table 2. Comparative performance of leukocyte detection over 80 images contaminated by Gaussian noise

Noise Level	Method	Leukocyte detected (True Positives)	Missing Leukocyte (False Negatives)	Wrongly Detected Leukocyte (False Positives)	True Positive Rate	False Positive Rate	False Discovery Rate	Positive Predictive Value
Gaussian Noise 463 Leukocytes σ= 10	HT	206	257	77	40.37%	18.07%	90.81%	72.79%
	FCCN	343	120	71	72.53%	16.67%	28.99%	82.85%
	GA+ACO	335	128	65	70.66%	15.26%	32.00%	83.75%
	PGSA	431	32	21	93.19%	4.93%	7.08%	95.35%

Table 3. Comparative performance of leukocyte detection over 80 images contaminated by salt and pepper noise

Noise Level	Method	Leukocyte detected (True Positives)	Missing Leukocyte (False Negatives)	Wrongly Detected Leukocyte(False Positives)	True Positive Rate	False Positive Rate	False Discovery Rate	Positive Predictive Value
Salt and Pepper Noise Level 10% 463 Leukocytes	HT	182	281	114	34.74%	26.76%	94.93%	61.49%
	FCCN	304	159	106	63.38%	24.88%	38.78%	74.15%
	GA+ACO	284	179	118	58.68%	27.70%	44.53%	70.65%
	PGSA	424	39	30	91.55%	7.04%	8.59%	93.39%

Thus, even under noisy conditions the PGSA is the most robust method to detect the leukocytes with the best detection rate, best positive predictive value, least false positive rate and the least false discovery rate.

Conclusion

In this paper, a new bionic random search algorithm has been proposed that makes use of the objective function's value as an input to the learning model while simulating a plant's phototropism for the automatic detection of WBCs embedded into complicated and cluttered smear images by considering it as a circle detection problem. The PGSA has been applied to solve this circle detection problem which gives the location of the WBCs in the images using three non-collinear edge points on the segmented edge map of the image as candidate circles. The resemblance of the encoded candidate circles to the actual WBC is evaluated by the

objective function. Based on the calculated value of the objective function, the set of encoded candidate circles (branch nodes) are evolved by using the PGSA so that they can fit into the actual blood cells that are contained in the edge map. The experimental results and the performance of the PGSA has been compared with other existing WBC detection algorithms which demonstrate the high performance of the proposed method in terms of detection accuracy, precision, sensitivity and noisy conditions. Although, there has been quite some research done to solve the circle detection problem when processing images, it has not been applied in the context of medical image processing. Moreover, PGSA has never been applied to solve such a problem. This evolutionary algorithm is highly efficient and is new to the field of computing intelligence. Thus, it offers a lot of scope for applications, implementations and further extension of this algorithm.

Acknowledgments

This work is a BK21 Plus project (SW Human Resource Development Program for Supporting Smart Life) funded by the Ministry of Education, School of Computer Science and Engineering, Kyungpook National University, Korea (21A20131600005).

References

Atherton, T. J. and Kerbyson, D. J. 1993. Using phase to represent radius in the coherent circle Hough transform. In Proceedings of the IEEE Colloquium on the Hough Transform, 269-278. IEEE, London

Ayala-Ramirez, V., Garcia-Capulin, C. H., Perez-Garcia, A, and Sanchez-Yanez, R. E. 2006. Circle detection on images using genetic algorithms. *Pattern Recognition Letters* 27(6):652– 657

Bhattacharjee, D. and Paul, A. 2016. A Hybrid Search Optimization Technique Based on Evolutionary Learning in Plants. In *Proceedings of 2016 Seventh International Conference of Swarm Intelligence*: 271-279. Bali, Indonesia: LNCS, Springer

Campi, C., Perasso, A., Beltrametti, M. C., Massone, A. M., Sambuceti, G., Piana, M. 2013. Pattern recognition in medical imaging by means of the Hough transform of curves. In Proceedings of Eighth IEEE International Symposium on Image and Signal Processing and Analysis (ISPA 2013):280-283

Chattopadhyay, K., Acharya. A., Banerjee, A., Basu, J., and Konar, A. 2008. Fast and Efficient Circle Detection Schemes for Digital Image. In Proceedings of First International Conference on Emerging Trends in Engineering and Technology. 128-133

Cuevas, E., Sención-Echauri, F., Zaldivar, D., and Pérez-Cisneros, M., 2012. Multi-circle detection on images using artificial bee colony (ABC) optimization. *Soft Computing*.16 (2): 281-296

Crepinsek, M., Liu, S., Mernik, M. 2013. Exploration and Exploitation in Evolutionary Algorithms: A Survey. *ACM Computing Surveys*. 45(3): Article 35(1-33)

Das, S., Dasgupta, S., Biswas. A., Abraham, A. 2008. Automatic Circle Detection on Images with Annealed Differential Evolution. In Proceedings of Eighth International Conference on Hybrid Intelligent Systems. September: 684-689

George, Y. M., Zayed, H. H., Roushdy, I., Elbagoury, B. M. 2014. Remote Computer-Aided Breast Cancer Detection and Diagnosis System Based on Cytological Images, *IEEE Systems Journal*. 8(3): 949-964

Isa, N., Sabri N. M., Jazahanim, K. S., Taylor, N.K. 2010. Application of the Clonal Selection Algorithm in artificial immune systems for shape recognition. In Proceedings of 2010 International Conference on Information Retrieval & Knowledge Management: 223-228

Karkavitsas, G., and Rangoussi, M. 2007. Object localization in medical images using genetic algorithms. *World Academy of Science, Engineering and Technology*. 2: 499–502

Muammar, H., and Nixon, M. 1989. Approaches to extending the Hough transform. In Proceedings of the International Conference on Acoustics, Speech, and Signal Processing (ICASSP '89), 3:1556–1559

Seo, S. W., and Kim, M. 2015. Efficient architecture for circle detection using Hough transform. In Proceedings of Sixth IEEE International Conference on Information and Communication Technology Convergence: 570-572

Shaked, D., Yaron, O., and Kiryati, N. 1996. Deriving stopping rules for the probabilistic Hough transform by sequential analysis. *Computer Vision and Image Understanding*. 63(3): 512–526

Tong, L., Wang, C., Wang, W., and Su, W. 2005. A global optimization bionics algorithm for solving integer programming-plant growth simulation algorithm. *Systems Engineering-Theory & Practice*. 25:76–85

Wang, C., Cheng, H. Z. 2007. A plant growth simulation algorithm and its application in power transmission network planning. *Automation of Electric Power Systems*. 31(7): 24–28

Wang, M., and Chu, R. 2009. A novel white blood cell detection method based on boundary support vectors. In Proceedings of IEEE International Conference on Systems, Man and Cybernetics (SMC '09), 2595–2598, San Antonio, Texas, USA

Wang, S., Korris, F. L., Fu, D. 2007. Applying the improved fuzzy cellular neural network IFCNN to white blood cell detection. *Neurocomputing*. 70(7-9):1348-1359.

Wu, J., Zeng, P., Zhou, Y., and Olivier, C. 2006. A novel color image segmentation method and its application to white blood cell image analysis. In Proceedings of the Eighth International Conference on Signal Processing (ICSP '06): 235-239

Yadav, V. K., Batham, S., Acharya, A. K., Paul, R. 2014. Approach to Accurate Circle Detection: Circular Hough Transform and Local Maxima Concept. In Proceedings of 2014 International Conference on Electronics and Communication Systems (lCECS -2014): 489-576

Zhou, X., Ito, Y., Nakano, K. 2014. An Efficient Implementation of the One-Dimensional Hough Transform Algorithm for Circle Detection on the FPGA. In Proceedings of 2014 Second International Symposium on Computing and Networking: 447-452

Zhaoxia, F., and Yan, H. 2012. A Circle Detection Algorithm Based on Mathematical Morphology and Chain Code. In Proceedings of 2012 International Conference on Computing, Measurement, Control and Sensor Network (CMCSN):253:256